Plasma Heating of Inert Gas Hollow Cathode Inserts

IEPC-2007-017

Presented at the 30th International Electric Propulsion Conference, Florence, Italy
September 17-20, 2007

Ira Katz,[*] Ioannis G. Mikellides,[†] Dan M. Goebel,[‡] and James E. Polk[§]
Jet Propulsion Laboratory, California Institute of Technology, Pasadena, CA, 91109

Abstract: We have developed a 2-D fluid model of the fundamental ionization and transport processes that occur inside electric propulsion hollow cathodes. Plasma fluxes to the internal cathode surfaces calculated by this model have been used as input to a simple hollow cathode thermal model. The thermal model predicts insert temperatures that are compared with fiber optic measurements. The 2-D fluid model gives unique insight into the relative importance of competing heating mechanisms in the plasma. It is shown that in hollow cathodes with a very small-diameter orifice, operating at a low current, the plasma density peaks inside the orifice, and the cathode is heated primarily by plasma bombardment in the orifice and along the orifice plate. As the orifice diameter increases, the peak plasma density moves upstream of the orifice, and ion and electron bombardment heat both the orifice plate and the insert. In hollow cathodes with a large-diameter orifice the plasma extends along much of the insert, the plasma density peaks well within the insert region, and the cathode is heated primarily by ion bombardment of the insert.

I. Introduction

INERT-gas-fed hollow cathodes are commonly used in ion and Hall thrusters to provide electrons for propellant ionization and beam neutralization. Depending on the thruster and the hollow cathode function, the cathodes in these devices operate over a wide range of electron currents and neutral gas flow rates. Over the past several years, computer simulations and detailed measurements of hollow cathode insert region plasma properties have lead to a clear understanding of how the thermionic emission insert is heated. While most of the cathodes studies had inserts made of the same low-work-function material and had the same physical dimensions, the insert plasma parameters, sheath potentials, and insert heating mechanisms varied as a function of cathode orifice diameter, gas flow rate, and electron current. We have developed a 2-D fluid model, OrCa2D,[1,2] of the fundamental ionization and transport processes that occur within these cathodes. The model has been validated with detailed laboratory measurements of the plasma parameters. Electron transport in the insert region is treated classically with a fluid model; no wave-particle enhancement is assumed in the plasma. Plasma fluxes to the internal cathode surfaces calculated by this model have been used as input to a simple hollow cathode thermal model.[3] The thermal model predicts insert temperatures that are compared with fiber optic measurements. The 2-D fluid model gives unique insight into the relative importance of competing heating mechanisms in the plasma. It is shown that hollow cathodes with an orifice of very small diameter, operating at a low discharge current, the location of the peak plasma density is inside the orifice, and the cathode is heated primarily by plasma bombardment within the orifice and along the orifice plate. As

[*] Group Supervisor, Electric Propulsion Group, 4800 Oak Grove Drive, Pasadena, CA, 91109, Mail Stop 125-109, Senior Member AIAA.
[†] Member Technical Staff, Electric Propulsion Group, 4800 Oak Grove Drive, Pasadena, CA, 91109, Mail Stop 125-109, Senior Member AIAA.
[‡] Section Staff, Thermal and Propulsion Engineering Section, 4800 Oak Grove Drive, Pasadena, CA, 91109, Mail Stop 125-109, Senior Member AIAA.
[§] Section Staff, Thermal and Propulsion Engineering Section, 4800 Oak Grove Drive, Pasadena, CA, 91109, Mail Stop 125-109, Senior Member AIAA.

the orifice diameter increases, the peak plasma density moves upstream of the orifice, and ion and electron bombardment heat both the orifice plate and the emitter insert. In a large-orifice hollow cathode, the plasma extends along much of the insert, the plasma density peaks well within the insert region, and the cathode is heated primarily by ion bombardment of the insert.

II. Types of Hollow Cathodes

Hollow cathodes generally fall into three categories, which will be useful later in describing the plasma characteristics in results below.[4] The first type of hollow cathode has a small orifice and a large length-to-diameter ratio, and is shown schematically in Fig. 1 as Type A. These cathodes typically operate at low current and relatively high internal gas pressures, and are heated primarily by orifice heating. In the second type of cathode the diameter of the orifice is typically larger than its length and is shown in Fig. 1 as Type B. Type-B cathodes usually operate at lower internal gas pressures. The heating mechanism(s) in these cathodes can be due to electron or ion bombardment of the insert, or by a combination of the two depending on the orifice size and operating conditions. Significant heating of the orifice plate by the plasma can also occur. The third type of cathode, typically used in high-current cathodes and shown in Fig. 1 as Type C, has essentially no orifice. These cathodes have a large neutral density gradient in the insert region and a lower internal pressure overall compared to orificed cathodes. The heating mechanism for Type-C cathodes is normally ion bombardment of the insert.

The neutral gas pressure inside the hollow cathode affects both the plasma density and plasma profile due to collisional effects. Figure 2 shows examples of axial plasma density profiles measured with fast scanning probes[5] inside a 0.38-cm (I.D.) cathode insert operating at 13 A of discharge current, and a xenon flow rate of 3.7 sccm. The profiles are compared for the three types of cathodes mentioned above. Small-diameter orifices, characteristic of Type-A cathodes, have high internal pressures that produce high plasma densities but constrain the axial extent of the plasma to the order of a few millimeters. For a given emission current density, this can restrict the discharge current that is available. As the orifice is enlarged, the pressure decreases and the plasma extends farther into the insert, resulting in utilization of more of insert surface area for electron emission.

Depending on the orifice size, the electron current density in the vicinity of the peak plasma density region is the highest of anywhere in the system and can easily exceed 1 kA/cm^2. If the orifice is long compared to its radius, as is the case in most Type-A neutralizer hollow cathodes, the physics are the same as in a classical positive column plasma where an axial electric field in the collisional plasma conducts the current, in which case, resistive heating in the plasma is very important. A large fraction of this ohmic power deposited in the orifice plasma goes into heating of the orifice plate by ion bombardment, which contributes to the insert heating by conduction and radiation. In Type-B cathodes the orifice is shaped nearly as an aperture and there is little local resistive heating. The plasma in the insert region is generated by ionization of the neutral gas and by the discharge current flowing through the insert region into the orifice. At high flow rates (and subsequent high plasma densities) in this type of cathode, insert heating is primarily by plasma electrons. At low flow rates or with large orifices the insert is heated predominately by ions bombarding the insert surface. In Type-C cathodes there is little or no orifice and the plasma couples from a collisionally-dominated region upstream inside the insert directly into the nearly collisionless cathode plume region. This creates long axial density and potential gradients and may expose some of the downstream region of the insert to higher potentials and ion bombardment. As is shown below, heating in this case is predominately by ion bombardment through the higher cathode sheath potential.

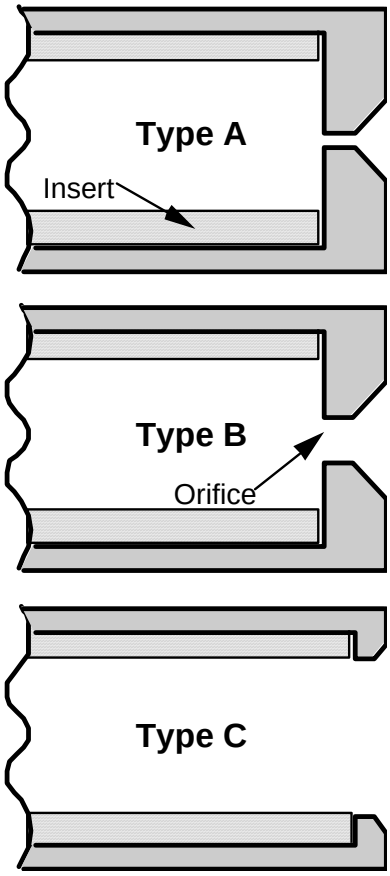

Fig. 1. Schematics of the three characteristic types of hollow cathodes (A, B and C) depending on the orifice geometry.

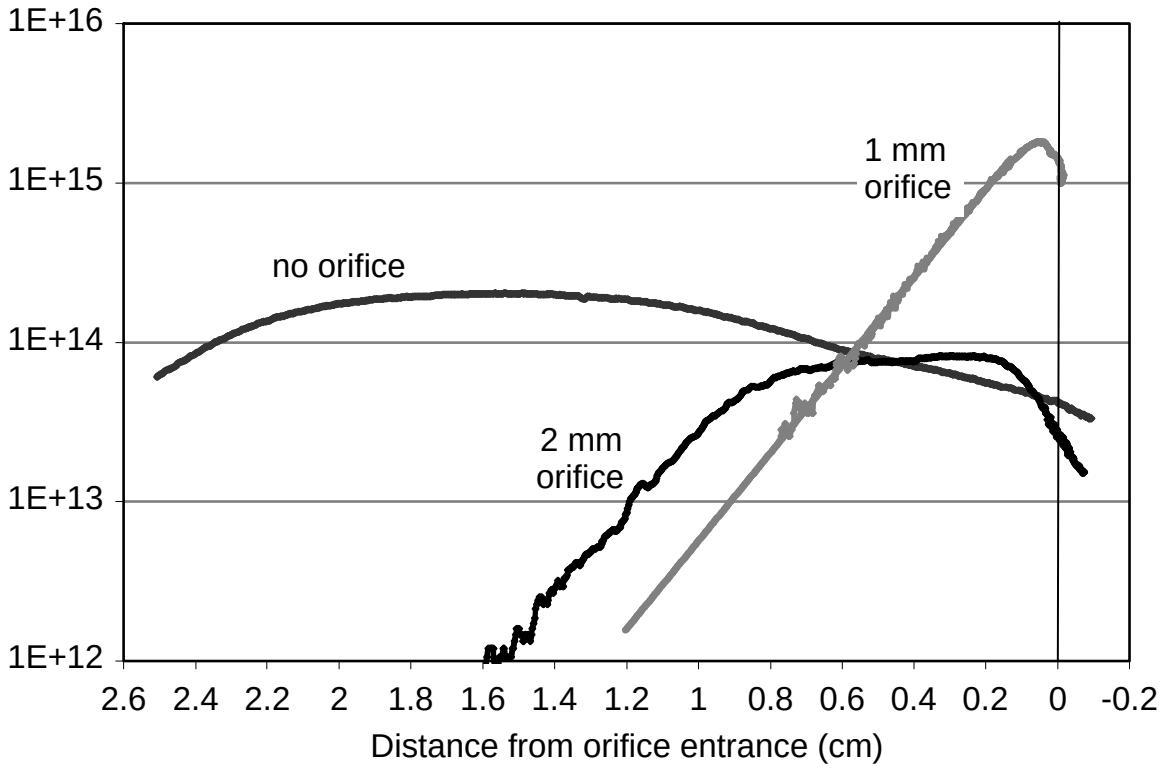

Fig. 2. Examples of plasma density (in #/m^3) profiles along the axis of symmetry in various cathodes as the orifice diameter is increased at fixed discharge current and gas flow.

Naturally, there is a continuous range of cathode operation that may demonstrate the properties of all three types of cathodes. Indeed, a given cathode geometry can transition from low resistive heating in the orifice at low currents and low gas flow rates to substantial resistive heating and plasma generation at high currents and high gas flow rates. Examples of the plasma conditions and heating mechanisms in these three types of hollow cathodes are presented below.

III. Thermal and Plasma Models

Computational models of the hollow cathode that have been developed at JPL include the 2-D Orificed Cathode (OrCa2D)[2] code and a 2-D thermal model.[3] The main motivation behind the development of OrCa2D is the assessment of keeper erosion and lifetime. In addition to the insert region, the computational region in OrCa2D includes the orifice channel and conical regions as well as the keeper and plume regions, as shown in Fig. 3. The plume region extends up to an anode boundary several centimeters downstream of the orifice. OrCa2D presently includes neutral gas dynamics, and is being developed to include all time-dependent terms that may be pertinent to ion acoustic and/or ionization oscillations. With an extended computational region that includes both the anode and cathode boundaries, and by including neutral gas dynamics, OrCa2D requires only knowledge of the cathode operating conditions (such as gas flow rate and discharge current) and insert temperature, but does not depend on experimental measurements of any of the plasma properties.

The 2-D thermal code uses the ion and electron fluxes from OrCa2D as input to predict the temperature distribution in the cathode. A sample problem geometry modeled by the thermal code is shown in Fig. 4. The positive numbers identify different materials, and negative numbers are used to identify radiative boundary conditions.

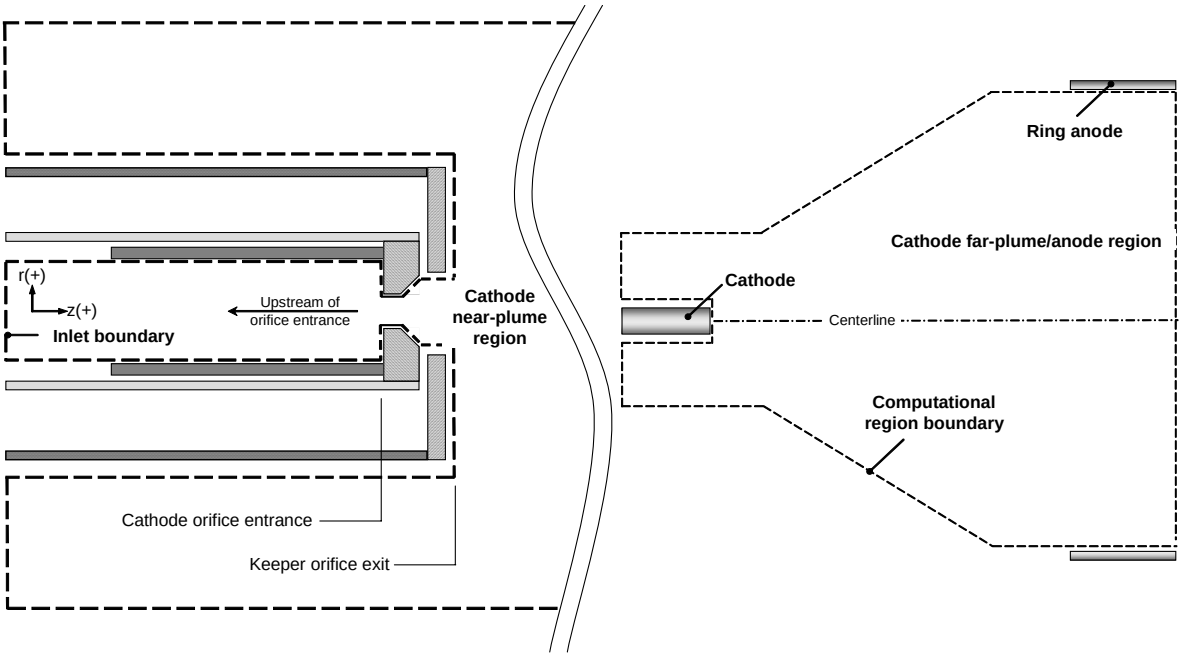

Fig. 3. Schematic of the hollow cathode outlining (by the dashed line) the computational region in OrCa2D. Left: Cathode interior and near-plume regions. The "near-plume" is defined as the region of plasma within a radius of a few centimeters downstream of the keeper orifice exit. Right: Far-plume/anode region.

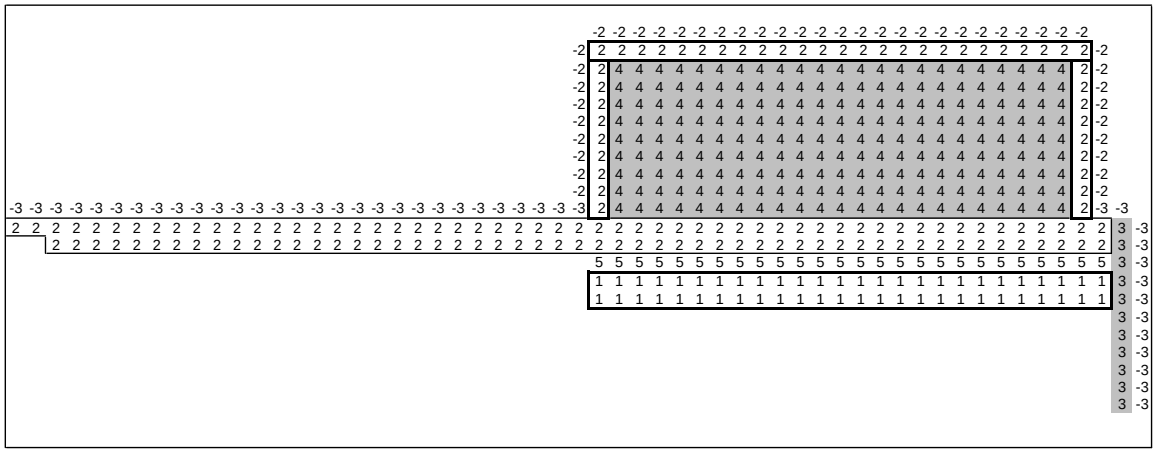

Fig. 4. Hollow cathode thermal model input geometry with the different types of cells numbered and the boundary conditions indicated by numbers. Negative numbers denote radiative boundaries.

The governing conservation laws of OrCa2D are solved in a time-split manner, and have been derived in detail by Mikellides *et al.* in Refs 1 and 2. We therefore provide only a brief description here. The electron and ion momentum equations, in the absence of the inertia terms, are added to yield the diffusive ion particle flux. The ion continuity equation is solved to yield the plasma density in the presence of ionization, which is determined based on measured ionization cross-sections. The neutral gas conservation equations for mass and momentum are solved for the neutral gas density and flux, and in the calculations presented herein the gas is assumed to be inviscid. Conservation of energy for the electrons gives the electron temperature, and includes thermal conduction of the electrons, work done by the electric field and loss of electron energy by ionization (inelastic) collisions. By assuming that ions and neutrals are in thermal equilibrium, a single equation is used for the conservation of energy of the heavy species, which provides the heavy-species temperature. Conservation of total current and Ohm's law for the electrons is solved for the plasma potential. In regards to the OrCa2D boundary conditions, both ions and

electrons are allowed to penetrate sheaths along walls and be absorbed by boundaries, including the insert sheath boundary. It is assumed that ions at wall-sheath boundaries attain the Bohm velocity. The absorbed electron current density follows the one-sided thermal flux assuming Boltzmann electrons. The emitted electron current density from the insert is modeled after the Richardson-Dushman equation for thermionic emission,[6] and includes the effect of the Schottky potential. The emitter temperature as a function of distance from the insert tip is set using a polynomial fit to measurements.[5] A model improvement proven critical by the NSTAR simulations with OrCa2D is emission enhancement under high plasma density conditions. The mechanism may be best characterized as "sheath funneling." The simulations suggested that in cathodes where the plasma density is high enough that the Debye length becomes smaller than the mean pore radius it is possible that the sheath penetrates into the pores, in the form of a "funnel", thereby enhancing the effective emission area. The enhancement is modeled using a multiplicative factor that that is inversely proportional to the Debye length and the ion-to-electron temperature ratio.[2]

A thermal model of the hollow cathode in r-z geometry has also been constructed. The model includes radiation and thermal conduction and receives inputs of the electron and ion fluxes to the cathode surfaces from OrCa2D. It then predicts the temperature distribution in the cathode. Figure 4 shows an example of a geometry used for prescribing "boundary types" in the thermal model. In Fig. 4, the positive numbers identify different materials, and negative numbers are used to identify radiative boundary conditions. The thermal model determines the heating of the cathode tube and insert due to power deposition in the orifice region, and accounts for thermal conduction and radiative heat losses, as well as radiative heat transfer within the emitter region.

An sample solution is shown in Fig. 5, which compares the predictions by the thermal code with measured temperatures of the insert for the NSTAR cathode operating at 12 A of discharge current. The code predicts an insert temperature of about 1210 ˚C in the first few millimeters away from the orifice plate where the plasma is in good contact with the insert. The combined plasma-thermal models showed the sensitivity of the hollow cathode temperature to the emissivity of the orifice plate, the thermal contact between the insert and the tube, and orifice heating (especially in neutralizer cathodes), all of which impact the performance and life of the cathode.

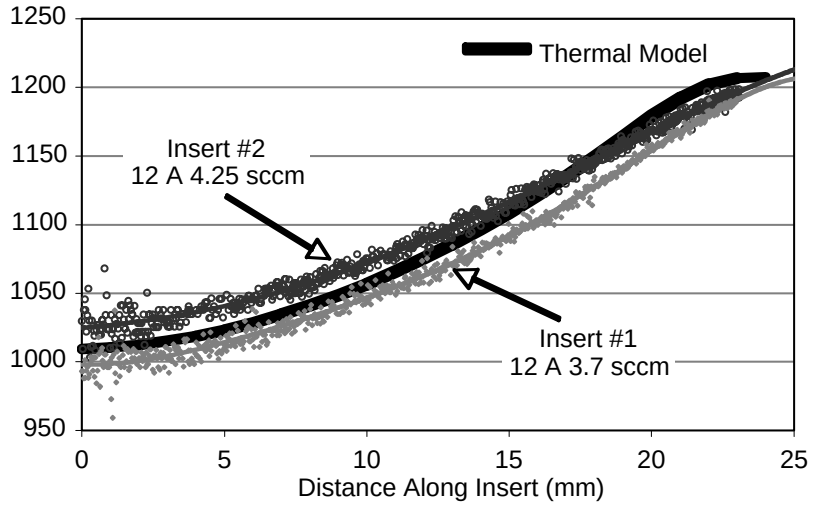

Fig. 5. Comparison of the measured and calculated temperature of insert in an NSTAR-like discharge cathode. The computed results were produced by the 2-D coupled thermal/plasma model.

IV. Model Results

Calculations were performed for three different cathodes and the results are presented in this section. The first set of calculations is for a Type-A hollow cathode, a cathode with a very small orifice diameter. The orifice and insert dimensions are roughly the same as those of the NSTAR neutralizer hollow cathode. The flow rate and current chosen are for one of the NSTAR thruster operating points. The second set of calculations is for a Type-B hollow cathode for which the orifice diameter is somewhat larger the orifice length. For this study a laboratory cathode was

chosen with orifice and insert dimensions roughly the same as those of the NSTAR discharge hollow cathode. Again the operating conditions were chosen to be the same as those of a typical NSTAR thruster operating point. The third set of calculations is for a Type-C hollow cathode, a cathode with a much larger orifice than either of the other two. The specific cathode was a laboratory device like the Type-B cathode, but with a larger orifice. The gas flow and current are chosen to compare directly with the NSTAR calculations. It is important to note that the Type-B and Type-C cathodes were not the same thermal design as the flight cathodes, but were laboratory devices constructed for ease of measuring internal plasma properties and insert temperatures.

Table 1. Hollow cathode operating conditions chosen for the numerical simulations.

Cathode	I_d (A)	Flow Rate (sccm)
Type A	3.26	3.59
Type B	15	3.7
Type C	15	3.7

Computed plasma densities for all three cathodes are shown in Fig. 6. The top plot shows the plasma density in a Type-A (small-orifice) hollow cathode. The plasma density peak occurs inside the orifice, and is 25 times and 130 times larger than the peak values in the Type-B and Type-C cathodes, respectively. Most of the plasma inside the Type-A cathode is generated as a result of resistive heating inside the orifice. The plasma density falls off very rapidly upstream, in the insert region. The middle plot in Fig. 6 shows the plasma density in a cathode with a somewhat larger orifice, a Type-B hollow cathode. The plasma density now peaks just upstream of the orifice, while the high-density plasma is in contact with both the orifice plate and the emitter insert. The bottom plot shows that in the case with the largest orifice, a Type-C hollow cathode, the plasma density peaks inside the insert region, well upstream of the orifice plate. In this case the power to generate plasma comes from the emitted electrons that are accelerated by the sheath potential. This is in contrast to Type-A (small-orifice) cathodes where ohmic heating in the orifice generates the plasma.

As is apparent from the plasma density plots, plasma heating occurs at different locations in each cathode. As shown in Table 2, in the Type-A cathode, almost all the heating occurs inside the orifice. This is obvious from the top plot in Fig. 6, since this is where almost all the plasma is located. As noted above, in the Type-B cathode the plasma is in roughly equal

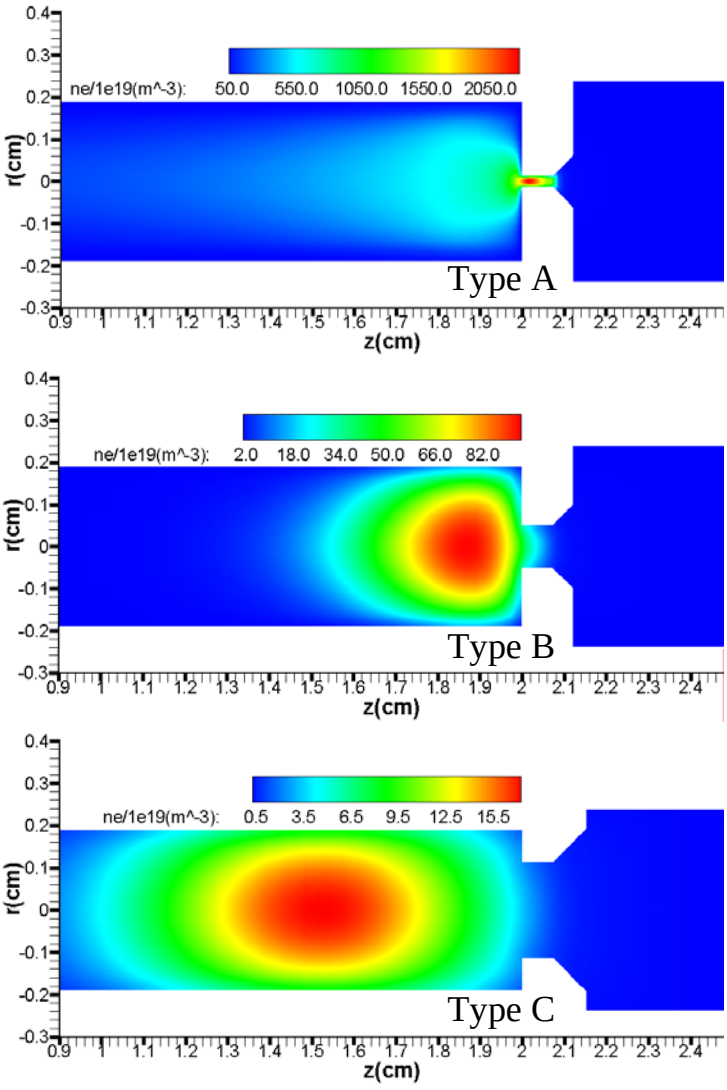

Fig. 6. Calculated plasma densities for the three cathode types.

contact with the orifice plate and the insert. Plasma heating is split between those two surfaces with very little heating taking place inside the orifice. It is noted that because in its present version the OrCa2D code includes the plume region (see Fig. 3), the fluxes for the Type-B cathode are quantitatively somewhat different from those previously reported for this cathode,[3] but qualitatively they are similar. The previously reported results[3] were based on the (only) version of OrCa2D available at the time (called then IROrCa2D) which excluded the orifice and plume regions. In the Type-C cathode the plasma peaks significantly upstream of the orifice plate, and as seen in Table 2, almost all of the heating occurs along the cathode insert. This progression of the heating upstream in the cathode as the orifice diameter increases is shown graphically in Fig. 7. Not only does the magnitude of the insert heating increase with orifice diameter but the location of the heating also moves. As shown in Fig. 8 the heating peaks very close to the orifice plate for the smallest orifice, Type-A cathode, and moves progressively upstream as the orifice increases in the Type-B and Type-C cathodes.

Table 2. Plasma heating in the three different cathodes.

Cathode	Region	Electron	Ion	Total
Type A	Emitter	-4.2	5.6	1.2
	Orifice Plate	0.73	3.19	3.9
	Orifice	0.55	18.44	19.0
Type B	Emitter	8.1	6.3	14.5
	Orifice Plate	13.5	3.3	16.8
	Orifice	1.3	1.0	2.3
Type C	Emitter	2.7	17.6	20.3
	Orifice Plate	1.0	0.4	1.4
	Orifice	0.3	0.2	0.5

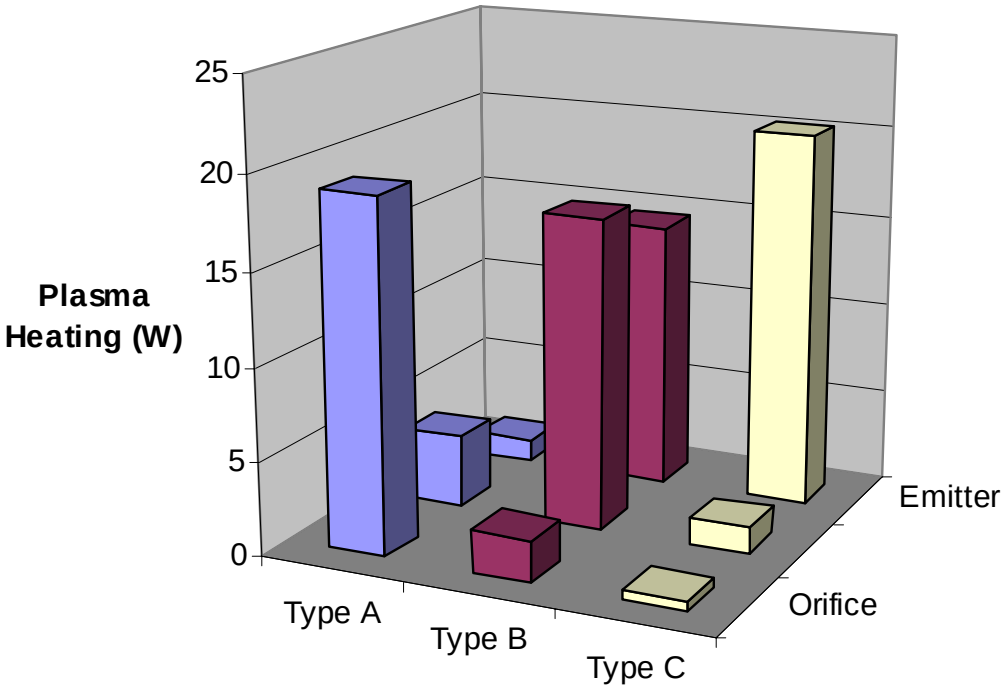

Fig. 7. The plasma heating moves from the orifice to the orifice plate to the insert as the orifice diameter increases.

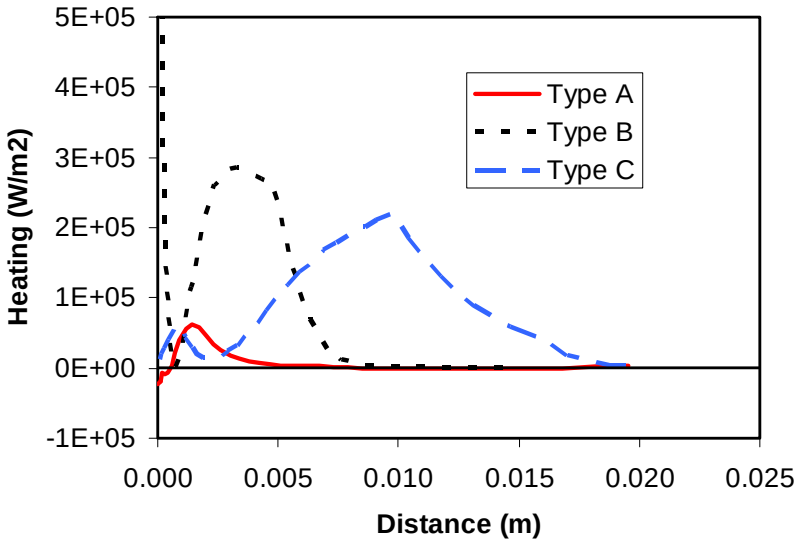

Fig. 8. The plasma heating extends for a longer distance down the insert as the cathode orifice increases.

The plasma fluxes shown in Fig. 8 were used as input to the cathode thermal model. The model parameters for the Type-B cathode were left unchanged from those reported in Ref. 3. For the Type-C cathode the orifice in the model was enlarged. For the small-orifice cathode (Type A), the orifice was reduced, and conductive heat loss to the base plate was eliminated to represent the insulator that would be present in a flight-like cathode. No insert thermal measurements were available for this cathode so the values shown are for illustrative purposes.

The computed insert temperatures are shown in Fig. 9. In the Type-A cathode the insert is found to be much cooler than either of the other cathodes. This is largely due to the fact that the almost all the available heating power is deposited into the orifice. The emitter is only heated by conduction and radiation from the orifice plate. The middle cathode, Type B, has both significant orifice plate and insert heating. As a result, its peak insert temperature is about 100° C hotter than the Type-C insert. The Type-C insert runs somewhat cooler than the Type-B cathode, consistent with lower total heating than the Type-B cathode. However, Types C and A both generate about 20 W of plasma heating, but in the Type-C cathode the power is deposited directly into the insert resulting in higher insert temperatures.

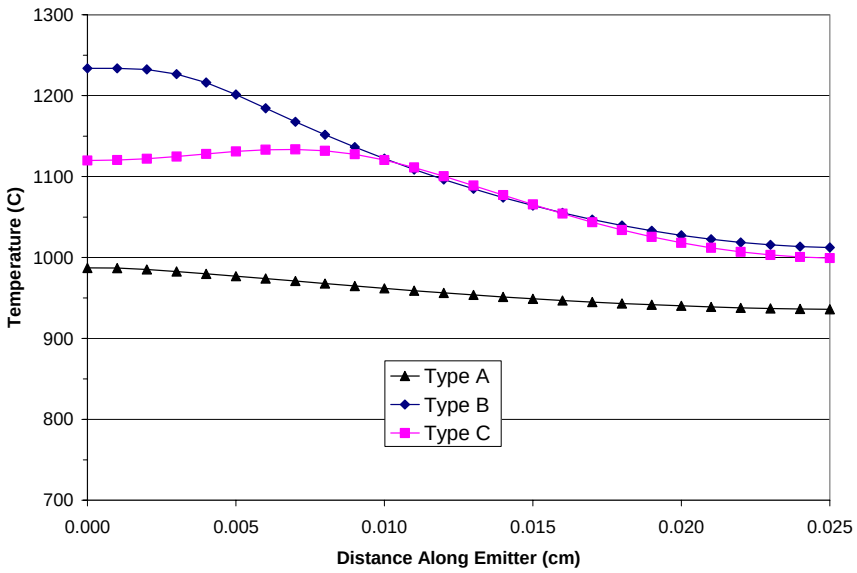

Fig. 9. Computed temperature profiles along the insert in the three cathode types.

V. Discussion

Plasma and thermal calculations were performed for hollow cathodes with three different orifice dimensions. In the Type-A (small-diameter orifice) cathode the plasma generation and heating was found to take place inside the orifice. The insert temperature was low since it receives only a fraction of the total heating power. This is consistent with published results of the NSTAR Extended Life Test (ELT),[7] where after more than 30,000 hours of operation, the neutralizer hollow cathode insert was in pristine condition.

The Type-B cathode, with a middle-sized orifice, was found to operate with the highest temperatures because both the insert and the orifice plate are heated. Published results from the NSTAR ELT showed that the discharge cathode insert showed substantial wear compared with the neutralizer hollow cathode.

The Type-C cathode had the largest orifice. It was found that the heat in this cathode was distributed along a substantial part of the insert. Very little heat was deposited in the orifice or along the orifice plate. This design promises long life for two reasons. First, the measured temperatures were substantially lower than the middle size orifice cathode. Based on published barium depletion rates in vacuum cathodes, every 40º C decrease results in a factor-of-two increase in life. Second, and often overlooked, the large orifice allows higher electric potentials inside the cathode making the cathode easier to ignite.

The combined plasma and thermal models represent a significant step forward in understanding the operation and life of hollow cathodes. Validation of hollow cathode life is one of the critical steps in qualifying electric thrusters for the long life and wide operating parameters needed for NASA's challenging deep space missions. With these models, the results of the NSTAR ELT can be used to predict the life of hollow cathodes on thrusters for NASA missions that use similar hollow cathodes, such as NASA's Evolutionary Xenon Thruster (NEXT)[8], L-3 Electron Technologies Inc.'s commercial Xenon Ion Propulsion System (XIPS),[9] and Aerojet's BPT-4000 Hall thruster.[10]

Acknowledgments

The research described in this paper was carried out by the Jet Propulsion Laboratory, California Institute of Technology, under a contract with the National Aeronautics and Space Administration in support of the In-Space Propulsion Technology Program.

References

[1] I. G. Mikellides, I. Katz, D. M. Goebel, and J. E. Polk, "Hollow Cathode Theory and Experiment, II. A Two-Dimensional Theoretical Model of the Emitter Region," *Journal of Applied Physics*, Vol. 98, No. 11, 2005, pp. 113303 (1-14).
[2] I. G. Mikellides, I. Katz, D. M. Goebel, and J. E. Polk, "Theoretical Model of a Hollow Cathode Plasma for the Assessment of Insert and Keeper Lifetimes," AIAA Paper 05-3667, July 2005.
[3] I. Katz, I. G. Mikellides, J. E. Polk, D. M. Goebel, and S. E. Hornbeck, "Thermal Model of the Hollow Cathode Using Numerically Simulated Plasma Fluxes," *Journal of Propulsion and Power*, Vol. 23, No. 3, pp. 522-527.
[4] J. E. Polk, A. Grubisic, N. Taheri, D. M. Goebel, R. Downey, and S. Hornbeck, "Emitter Temperature Distributions in the NSTAR Discharge Hollow Cathode", AIAA Paper 05-4398, July 2005.
[5] D. M. Goebel, K. K. Jameson, R. Watkins, and I. Katz, "Cathode and Keeper Plasma Measurements Using an Ultra-Fast Miniature Scanning Probe," AIAA Paper 04-3430, July 2004.
[6] S. Dushman, "Electron Emission from Metals as a Function of Temperature," *Phys. Rev.*, Vol. 21, No. 623, 1923.
[7] A. Sengupta, J. R. Brophy, J. R. Anderson, C. Garner, B. Banks, and K. Groh, "An Overview of the Results from the 30,000 Hr Life Test of Deep Space 1 Flight Spare Ion Engine," AIAA Paper 04-3608, July 2004.
[8] M. J. Patterson, and S.W. Benson, "NEXT Ion Propulsion System Development Status and Performance," AIAA Paper 07-5199, July 2007.
[9] W. Tighe, K. Chien, E. Solis, P. Robello, D. M. Goebel, and J. S. Snyder, "Performance Evlauation of the XIPS 25-cm Thruster for Application to NASA Missions," AIAA Paper 06-4999, July 2006.
[10] K. de Grys, B. Welander, J.Dimicco, , S. Wenzel, B. Kay, V. Kayms, and J. Paisley, "4.5 kW Hall Thruster System Qualification Status," AIAA Paper 05-3682, July 2005.